AN ABSTRACT OF THE THESIS OF

Jennifer E. Johnson for the degree of Master of Science in Radiation Health presented on June 8, 1994.

Title: The Use of ^{60}Co Cell Survival Curves in BNCT Research

Abstract approved: Redacted for Privacy

Stephen E. Binney

The cell survival curve is the only means by which to both qualitatively and quantitatively assess morphologic alterations directly resulting from *in vitro* irradiation of the cell. A ^{60}Co cell survival curve experiment has successfully demonstrated the response of the AtT-20 clone mammalian cell line to the effects of gamma rays. With the results of this experiment, a low LET radiation cell survival curve now exists to be used as a comparative upon the completion of BNCT cell survival curves.

The Use of ^{60}Co Cell Survival Curves in BNCT Research

by

Jennifer E. Johnson

A THESIS

submitted to

Oregon State University

in partial fulfillment of
the requirements for the
degree of

Master of Science

Completed June 8, 1994

Commencement June 1995

APPROVED:

Redacted for Privacy

Professor of Nuclear Engineering in charge of major

Redacted for Privacy

Head of Department of Nuclear Engineering

Redacted for Privacy

Dean of Graduate School

Date thesis is presented: June 8, 1994

Typed by: Jennifer E. Johnson

ACKNOWLEDGEMENTS

Much of the credit for the completion of this thesis is due to many individuals without whose support financially, academically, and emotionally, it would not have been possible.

First, I would like to thank Dr. Steve Binney (OSU) who initially agreed to allow me to be a part of the BNCT project, without which I would not have been able to afford graduate school. The amount of experience this project has given me, (both research and otherwise), is immeasurable, thanks for your patience and guidance.

Second, I would like to say thanks to all those who helped with the research and experimental procedures. Without the help of the Radiation Center staff and the Oregon Health Sciences crew (specifically Dr. Barry Albertson and Dr. Monica Millan), this project would never have survived. More directly I would like to thank Steve Martsolf for the incredible amounts of help I enthusiastically recieved for each experiment. It is much appreciated. Thank you as well to another co-worker Chris Vostmyer, who helped immensely with several calculations.

Third, thanks to all committee members, (Dr. John Ruben, Zoology; Dr. Jack Higginbotham, Nuclear Engineering; Dr. Victor Madsen, Physics), I appreciate the time and effort each of you put forth.

Finally, I would like to say that without the support of my family and friends, this would have been a more difficult process. I would especially like to thank my parents, Art and Jane Johnson, who gave me the drive and support to achieve my goals.

TABLE OF CONTENTS

LIST OF FIGURES

LIST OF TABLES

The Use of ^{60}Co Cell Survival Curves in BNCT Research

CHAPTER 1. INTRODUCTION AND LITERATURE REVIEW

The primary goal of any cancer radiation therapy is to kill tumor cells by introducing lethal doses of radiation to the cancerous tissues, ideally to every cancer cell. However, there are many drawbacks to the conventional type of radiation therapy. Traditional radiation therapy involves a beam of radiation (usually X-rays or soft gamma-rays) that is aimed at the tumor location from *outside* the body. Although this type of radiation is very effective at killing cancer cells, it is also very proficient at killing healthy cells. Therefore, due to the type of radiation used in conventional therapy and the relatively nonspecific manner in which the radiation is delivered, healthy tissues are damaged and the patient's whole body dose of radiation is often very high. In addition, the treatment is generally repeated several times, and there is still no guarantee that every cancer cell received a lethal dose of radiation.

An ideal type of radiation therapy for cancer would preferentially kill all tumor cells, while not seriously damaging healthy tissues. Incredibly, the concept for this type of therapy has existed for over fifty years in a reaction known as boron neutron capture. The reaction involves a ^{10}B atom which when bombarded by a thermal or epithermal (i.e., low energy) neutron, promptly disintegrates into a ^{7}Li nucleus and a stripped helium nucleus, otherwise known as an alpha particle. An average of 2.34 MeV of energy is released per event within a distance of 10 microns. From this reaction was developed boron neutron capture therapy (BNCT), an alternative form of radiation therapy.

The method of BNCT as a cancer treatment therapy involves loading boron-10 atoms into tumor cells and subsequently irradiating the area with thermal or epithermal neutrons. This type of therapy is seen as being primarily used for inoperable tumors, especially in the brain where the sparing of healthy tissue is of extreme importance. In order for BNCT to be successful, a critical amount of ^{10}B and a sufficient number of thermal or epithermal neutrons must be delivered to individual tumor cells.

BNCT research at Oregon State University (OSU) with the collaboration of researchers at Oregon Health Sciences University (OHSU) has focused on cancers of the endocrine system, specifically pituitary tumors. This research involves the *in vitro* irradiation of boron-infused rat pituitary cancer cells, with subsequent reculture and observation. This study addresses the importance of the cell survival curve as a means of measuring the response of the cells to varying doses of radiation, and successfully demonstrates the classic response of mammalian cells when exposed to varying doses of ^{60}Co radiation.

Topics presented will include a brief background and history of BNCT, including some treatment possibilities and future considerations, an explanation of cell survival curves and their role in radiobiologic studies, and the application of cell survival curves in the OSU BNCT program.

1.1 BNCT: Past, Present and Future

Enrico Fermi and his associates first noted in 1934 that if neutrons were slowed by passage through paraffin or water, they were more likely to be absorbed by atomic nuclei [1,2,3,4]. On December 10, 1934 the first observation of charged particles from

slow neutron irradiation was made at Cambridge University [5]. When these neutron capture reactions became known in the United States, it was proposed that they be applied to radiation therapy by the selective uptake of a suitable isotope into a patient's tumor, followed by slow-neutron irradiation of the tumorous tissue [6]. Although these nuclear reactions were found to occur with ^{10}B, ^{7}Li and nitrogen, boron was the chosen element since it not only could be incorporated into various tumor-affinitive drugs, but was also the most likely to react with a neutron in a slow neutron field [7]. By using radium mixed with a beryllium powder as a neutron source, the first radiobiologic studies using the ^{10}B neutron reaction were performed at the University of Illinois in 1938 [8]. During the next few years there were various claims of the reduced viability of mouse tumor transplants and the regression of mouse sarcomas after exposure to boric acid and subsequent *in vitro* slow neutron irradiation [8] .

After World War II, circumstances in the United States were appropriate for studies in radiobiology and medical physics to begin at institutes such as Brookhaven National Laboratory (BNL), established by the Atomic Energy Commission (AEC) for primarily non-military nuclear physics research [9]. These studies included a renewed interest in neutron capture therapy. In August of 1950 the Brookhaven Graphite Research Reactor (BGRR) was commissioned, and soon afterwards plans began for an irradiation facility to be built at the top of the BGRR. This facility would include a neutron port with a major intermediate (epithermal) energy component in the neutron beam specifically for BNCT [9]. Beginning in 1951, some patients with glioblastoma multiforme were referred to Brookhaven for BNCT at the irradiation facility of the BGRR [9].

The first patient was irradiated at the BGRR on February 15, 1951, just six months after the BGRR was commissioned [9]. Although no serious side effects from the BNCT were seen in the first set of ten patients, the therapy itself was largely unsuccessful. The second and third BNCT trials still showed little or no therapeutic efficacy, with a median post-therapy survival time of 96 days. The researchers concluded that the boron compounds did not concentrate and persist in the tumor cells and the thermal neutrons did not penetrate to adequate depths [10].

In 1958, research began at the Massachusetts Institute of Technology (MIT) to identify a ^{10}B carrier that yielded more favorable tumor:brain boron concentration ratios [9]. A p-carboxyl derivative, which showed a 2.5-9.0 tumor-to-tissue ratio between 15 minutes and 3 hours after intraperitoneal injection, was selected as a ^{10}B carrier in 16 patients treated with BNCT at the MIT reactor. This outcome, like others, was unsatifactory in that the median survival time was only six months [11].

In these early clinical trials with BNCT, it was discovered that a major complication was radiation damage to the cerebral vasculature. This was due in part to the fact that no technique existed that was fast enough to allow estimation of a patient's blood ^{10}B concentration in planning the irradiation time [9]. In addition, few boron-containing compounds existed that would enter the glioma freely, while not crossing the blood-brain barrier. Boron compounds specifically for this purpose were first synthesized in the 1960s from polyhedral boranes [12,13]. After studies demonstating the applicability of these types of compounds, sodium mercaptoundecahydrododecaborate (commonly known as BSH) was selected for a trial of BNCT for brain tumors in Japan

[9]. The first BNCT irradiation in Japan took place in August of 1968 [14]. Since that time there have been reports of excellent clinical results in some malignant glioma patients treated with BNCT in Japan [9]. One man treated with BNCT at age 50 in 1972, was alive and neurologically stable in the spring of 1990 (Hatanaka 1990, unpublished). Even with this and other successes, the western world is reluctant to adopt the Japanese techniques in favor of refining and improving some of the methods. Many of the techniques used in Japan tend to require many hours of irradiation and involve some trauma to the skull of the patient.

Another area of special interest involves the development of compounds that might serve in the treatment of malignant melanoma [10]. Melanomas tend to incorporate elevated levels of phenylalanine, an essential amino acid, into the pigment melanin. Researchers are therefore attempting to develop phenylalanine derivatives that contain boron in hope that the melanoma cells would incorporate the boronylated compound [10].

A related technique relies on the fact that malignant cells tend to uptake nucleosides, the building blocks of DNA, at a faster rate than do normal cells [10]. One key advantage of concentrating the boron in the nucleus of the cell is that it would greatly enhance the destructive effects of the α-particles [10].

The use of antibodies as "guided missiles" is another approach to the delivery of ^{10}B. Antibodies are proteins that have the ability to recognize specific antigens on the surfaces of tumor cells [10]. Monoclonals, a highly specialized form of antibodies, were quickly recognized as having the greatest potential in boron delivery for a variety of tumor-killing agents [10].

It has also been discovered that heavy water, or D_2O may actually improve the mechanism of BNCT through partial deuteration of tissues being considered for the therapy. In preliminary experiments, brain water deuteration has allowed improved thermal neutron transmission with reduced capture γ ray doses due to the lower cross section of D_2O as compared to H_2O [15]. This method is thought to have promise for deep-seated or wide-spread tumors.

Current BNCT research focuses mainly on identifying pharmacologically and radiobiologically suitable boron carriers. One of the most recent advances in boron carriers is being researched at OHSU and OSU for the treatment of pituitary tumors. The carrier molecule is a hypothalamic polypeptide releasing hormone known as ovine corticotrophin releasing hormone (oCRH). A $^{10}B_{10}$ carborane cage (synthesized, purified and supplied by Professor M. Frederick Hawthorne, Department of Chemistry and Biochemistry, UCLA) is then attached to the oCRH using polypeptide bonds. [16]

1.2 The Boron Neutron Capture Reaction

Boron neutron capture therapy is based on the reaction that occurs when ^{10}B (stable) is bombarded with a thermal neutron to yield highly ionizing stripped down helium nuclei (α-particles) and ^{7}Li nuclei.

$$^{10}B + n_{th}\,(0.025\text{ eV}) \rightarrow [^{11}B] \rightarrow \begin{cases} ^{4}He + {}^{7}Li + 2.79\text{ MeV}\ (6\%) \\ ^{4}He + {}^{7}Li + 0.48\text{ MeV}\ \gamma + 2.31\text{ MeV}\ (94\%) \end{cases}$$

From these two reaction pathways, it is possible to note the high energy release of 2.79 MeV 6% of the time and 2.31 MeV 94% of the time, with a weighted average energy emission of 2.34 MeV per capture reaction. As can be noted, most (83%) of the energy released can be attributed to the ^{7}Li nucleus and the α-particle, while the remaining 17% of the energy released is due to a prompt γ-ray. Since the particles released are high LET (Linear Energy Transfer), they give rise to closely spaced, highly ionizing events which destroy a wide variety of biologically active molecules including DNA, RNA and proteins [17]. Figure 1-1 illustrates the mechanics of this reaction as it occurs inside of a tumor cell.

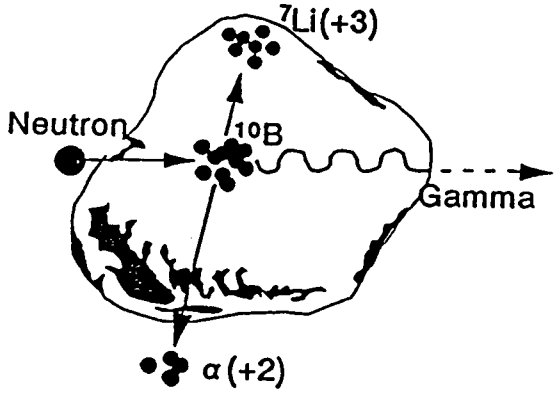

Figure 1-1 BNCT Reaction Inside A Tumor Cell
A ^{10}B nucleus generating an α-particle and a 7Li nucleus, both high LET particles capable of killing the cell.

There are a number of nuclides with a high propensity to absorb thermal neutrons (Table 1). This property is known as the neutron cross section, symbolized as σ, and is measured in barns ($1b = 10^{-24}cm^2$). ^{10}B was chosen as the nuclide of choice for the following reasons: (a) it is nonradioactive, comprises 20% of all natural boron, and is readily available, (b) the particles released are largely high LET, (c) unlike x-rays, α-particles do not require oxygen to enhance their biological effectiveness, which is particularly useful since a rapidly expanding tumor often outgrows its blood supply [10], and (d) ^{10}B can be incorporated into a variety of radiobiologically and pharmacologically useful structures [17].

Table 1-1 Thermal neutron capture cross section values of potential nuclides for neutron capture therapy

Nuclide	Cross-section (σ)†	Nuclide	Cross-section (σ)†
^{3}He	5,500	^{155}Gd	58,000
^{6}Li	953	^{157}Gd	240,000
^{10}B	3,837	^{174}Hf	400
^{113}Cd	20,000	^{199}Hg	2000
^{135}Xe*	2,720,000	^{235}U*	678
^{149}Sm	41,500	^{241}Pu*	1,375
^{151}Eu	5,900	^{242}Am*	8,000

* Indicates that the nuclide is radioactive

† Capture cross-sections are given in barns ($1b = 10^{-24}$ cm^2)

Table 1-2 Thermal neutron capture cross section values of normal tissue elements

Element	Cross-section (σ)†	Element	Cross-section (σ)†
H	**0.332**	**N**	**1.75**
Na	0.536	P	0.19
K	2.07	O	<0.0002
Mg	0.069	S	0.52
Ca	0.44	Cl	33.8
C	0.0037	Fe	2.62

†Capture cross-sections are given in barns (1b = 10^{-24} cm^2)

Some nuclides of elements in normal tissues also tend to absorb thermal neutrons (Table 2). This poses a slight problem even though these elements have a cross section several orders of magnitude lower than boron. Two of these elements, hydrogen and nitrogen, are present in such high concentrations that their capture neutrons contribute significantly to the total radiation absorbed dose [17]. This effect can be extremely detrimental to the delicate vasculature of the brain. It is possible to reduce this by ensuring the tumor have extremely high ^{10}B concentrations so that the neutron fluence (n-cm^{-2}) can be kept relatively low, thereby maximizing the $^{10}B(n,\alpha)^7Li$ reaction while the (n,p) reaction with nitrogen [$^{14}N(n,p)^{14}C$] and the (n,γ) reaction with hydrogen [$^1H(n,\gamma)^2H$] can be kept to a minimum [17]. It has been estimated that for ^{10}B in tumor tissue at concentration of 50 μg/g, 86% of the dose would be from the ^{10}B capture reaction [17]. The necessary concentration has also been stated as 10^9 (1 billion) ^{10}B atoms per cell, a number which was derived from experiments performed up to two decades ago, which defined the "minimal tumoricidal concentration" of ^{10}B in wet tissue samples to be 15-50

μg/g, [10,17] but should not exceed 100 μg/g to avoid the self-shielding effect of boron at high concentrations [15].

1.3 Boron Quantification Techniques

In order for BNCT to be successful, it is necessary to be able to quantitate the amount of boron in the tumor cells. Two techniques recently introduced are Inductively Coupled Plasma Atomic Emission Spectroscopy (ICP-AES) and Inductively Coupled Plasma Mass Spectroscopy (ICP-MS). These methods are capable of measuring boron in samples with a precision of 3% at levels of 0.15 ppb, and a precision of 1% at higher levels [18]. The only drawback to methods such as these is that there is no way to determine where in the cell the boron is located. However, it is by far the most sensitive technique for measuring low levels of boron and some other elements.

ICP-MS is the method used to quantify levels of boron in the cellular studies at OSU. This is in part due to the new facility locally available at the OSU College of Oceanography and Atmospheric Sciences. ICP-MS embodies two technologies, ArICP and quadrupole mass spectroscopy, each of which has existed for over three decades [19]. ArICP was best known as an emission source for multi-element spectroscopic analysis. Organic mass spectroscopy has shown great successes by applying quadrupoles as the impetus to improved performance characteristics [19].

In ICP-MS samples are generally introduced in aqueous solutions. Samples are then peristaltically pumped through a nebulizer which then breaks the sample into an aerosol with droplets a few hundred μm in diameter. Since the maximum droplet size that can be completely desolvated, atomized and ionized in its course through the plasma

is about 10μm, the aerosol is subsampled through a spray chamber. (This amounts to approximately 1% of the sample reaching the plasma, with the rest being pumped to waste.) The plasma is lit by momentarily discharging a spark coil, which strips electrons from the gas entering the chamber, and reaches 10,000°C. The ions are then directed from the plasma into the quadrupole detection system, which consists of four parallel rods to which AC and DC voltages are applied. Ions of a chosen charge-to-mass ratio preferentially oscillate in the plane parallel to the rods and strike the detector. The voltages are set so that signals are resolved to 1 amu. Signals reaching the electron multiplier are then amplified and sent to a multichannel analyzer and processed by computer [19]. Due to the ingeneous ion extraction system, the relative ion count rates directly reflect the composition of the sample [20].

Complications occur when this technique is applied to biological tissue, primarily due to the "stickiness" of the cell membranes. Sample digestion is therefore necessary and is achieved through a method known as closed vessel microwave digestion. However, unless sample digestion is complete, a precipitate can form, causing lower values for the analyte concentration [21].

1.4 BNCT as a Treatment For Pituitary Tumors

Pituitary tumors are a type of endocrine cancer that because of certain characteristics make them excellent candidates for BNCT. Since the pituitary gland itself is approximately 1 cm in diameter, tumors of this organ tend to be less than 2 cm in diameter and very localized. In addition, the mechanism of ^{10}B transport allows for increased specificity since each tissue of the endocrine system contains cellular membrane

receptors which bind and internalize only appropriate releasing hormones. Therefore, specifically tagged molecules would be recognized and subsequently delivered to the desired area.

Although not always malignant, pituitary tumors comprise approximately 10-15% of all intracranial tumors [22]. These tumors, even when benign, generally cause large amounts of certain hormones to be released from the pituitary, and are associated with such disorders as acromegaly (Growth Hormone, [GH]), Cushing's disease (Adrenocorticotropin Hormone, [ACTH]), and thyrotoxicosis (Thyroid Stimulating Hormone, [TSH]). These disorders cause many physically distressing symptoms; however, rarely are they fatal.

The pituitary gland sits at the base of the brain in a small indentation of cranial bone called the *sella tursica* (see Figure 1-2). The anterior lobe of the pituitary gland (adenohypophysis) contains specific secretory cells for several vital hormones. Directly above and connected to the pituitary is the hypothalamus, which is responsible for secreting *releasing hormones* specific to each of the hormones produced in the pituitary. In order for a hormone to be released from the pituitary, a secretory cell must successfully recognize and bind with its specific releasing hormone. By "tagging" specific releasing hormones with ^{10}B, it is possible to load boron very specifically into cells of the pituitary.

Experiments to demonstrate the efficacy of this method are being carried out at OSU in collaboration with researchers from OHSU. A synthetic "boronylated" releasing

hormone was manufactured consisting of a $^{10}B_{10}$ (ten-atom) carborane cage attached by way of polypeptide bonds to oCRH (ovine corticotropin releasing hormone).

It should be noted that a fairly clear route for surgical removal exists directly through the *sphenoidal sinus*, and has been successful. However, BNCT allows for a completely specific and unintrusive removal.

Although conditions resulting from pituitary tumors are generally more distressing than fatal, many other endocrine cancers, such as breast, prostate, pancreatic and adrenal, tend to be quite metastatic and often fatal. It is therefore hoped that by studying the effects of BNCT on a typical endocrine tissue, i.e., pituitary cells, much will be learned concerning other more lethal types of endocrine cancers.

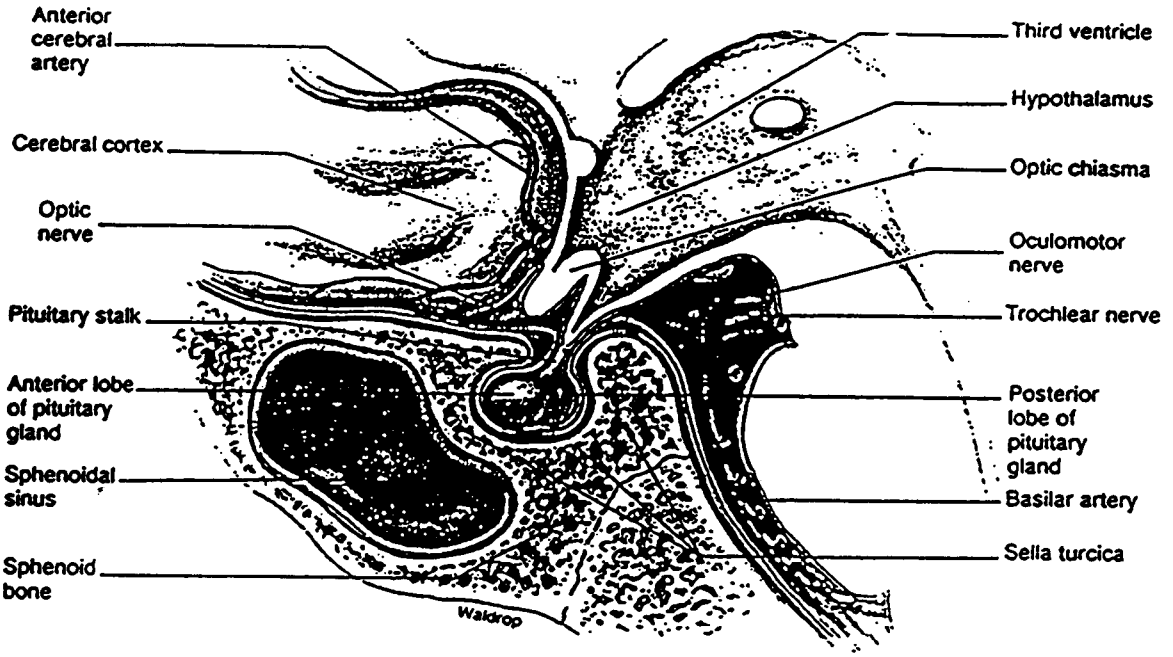

Figure 1-2 The Pituitary Gland

1.5 References

1. Fermi, E., Amaldi E., D'Agostino O., Rasetti F., Segre, E., (1934), "Artificial radioactivity produced by neutron bombardment," *Proceedings of the Royal Society of London*, A, **146**, 483-500.

2. Fermi, E., (1939), "Artificial radioactivity produced by neutron bombardment," In: *Les Prix Nobel en 1939*. Edited by M.A. Holmberg, Stockholm: Norstedt and Soner.

3. Amaldi, E., D'Agostino, O., Fermi, E., Pontecorvo, B., Rasetti, F., Segre, E., (1935), "Artificial radioactivity produced by neutron bombardment" - II. Proceedings of the Royal Society of London, A., **149**, 522-558.

4. Stranathan, J.D., (1942), *The 'Particles' of Modern Physics*, New York: Blakiston, pp. 386-402.

5. Goldhaber, M., (1986), Introductory remarks, In: *Proceedings of a Workshop on Neutron Capture Therapy*, Reports BNL-51994, Edited by R.G. Fairchild and V.P. Bond, Upton, NY: Brookhaven National Laboratory, pp. 1-2.

6. Locher, G.L., (1936), "Biological effects and therapeutic possibilities of neutrons," *American Journal of Roentgenology*, **36**, 1-13.

7. Farr, L.E., Robertson, J.S., (1971), "Neutron capture therapy," In: *Handbuch der Medizinische Radiologie*, Heidelberg: Springer, pp. 68-92.

8. Kruger P.G., (1940), "Some biological effects of nuclear disintegration products on neoplastic tissue," *Proceedings of the National Acadamy of Sciences of the USA*, **26**, 181-192.

9. Slatkin, D.N., "A History of Boron Neutron Capture Therapy Of Brain Tumors," *Brain*, **114**, 1991, pp. 1609-1629.

10. Barth, R.F., Soloway, A.H., Fairchild, R.G., "Boron Neutron Capture Therapy for Cancer," *Scientific American*, Oct. 1990, pp. 100-106.

11. Hatanaka, H., (1986), Introduction, In: *Boron-Neutron Capture Therapy for Tumors*, Edited by H. Hatanaka, Niigata, Japan: Nishimura, pp. 1-28.

12. Miller, H.C., Miller N.E., Muetterties, E.L., (1963), "Synthesis of polyhedral boranes," *Journal of the American Chemical Society*, **85**, 3885-3886.

13. Knoth, W.H., Sauer, J.C., England, D.C., Hertler, W.R., Muetterlies, E.L., (1964), Chemistry of borons, XIX. Derivative chemistry of $B_{10}H_{10}^{-2}$ and $B_{12}H_{12}^{-2}$, *Journal of the American Chemical Society*, **86**, 3973-3983.

14. Hatanaka, H., Urano, Y., (1986), Eighteen autopsy cases of malignant brain tumors treated by boron neutron capture therapy between 1968 and 1985. In: Boron Neutron Capture Therapy for Tumors, Edited by H. Hatanaka, Niigata, Japan: Nishimura pp. 381-416.

15. Matsumoto, T., "Transport Calculations of the Influence of Physical Factors on Depth-Dose Distributions in Boron Neutron Capture Therapy," *Physics, Medicine and Biology*, **35**, 1990, pp. 971-978.

16. Albertson, B. D., Millan M. A., Binney S. E., Willeke, G. B., Martsolf S. W., Johnson, J. E., Loriaux, D. L., "The Use of Boron Neutron Capture for the Treatment of Pituitary Tumors," *Advances in Neutron Capture Therapy*, edited by A.H. Soloway *et al.*, 1993, pp. 623-628.

17. Barth, R.F., Soloway, A.H., Fairchild, R.G., "Boron Neutron Capture Therapy for Cancer," *Cancer Research*, 50, 1990, pp. 1061-1070.

18. Gregorie, D.C., "Determination of Borons in Fresh and Saline Waters by Inductively Coupled Mass Spectrometry," *Journal of Analytical Atomic Spectrometry*, vol. 5, Oct. 1990, pp. 623-626.

19. Ungerer, A., A Description of ICP-MS, College of Oceanography and Atmospheric Sciences, Oregon State University, 1993.

20. Durrant, S.F., "Inductively Coupled Plasma-Mass Spectroscopy for Biological Analysis," *Trends in Analytical Chemistry*, II, 1992, pp. 73.

21. Campbell, M.J., Vermeir, G., Dams, R., "Influence of Chemical Species on the Determination of Mercury in a Biological Matrix (Cod Muscle) Using Inductively Coupled Plasma Mass Spectrometry," *Journal of Analytical Atomic Spectrometry*, vol. 7, June, 1992, pp. 617-621.

22. Thapar, K., Kovacs, K., Laws, E.R., Muller, P.J., "Pituitary Adenomas: Current Concepts in Classification, Histopathology, and Molecular Biology," *The Endocrinologist* 3(1): 39-57, 1993.

CHAPTER 2. CELL SURVIVAL CURVES

2.1 Explanation and Purpose

A cell survival curve describes the relationship between the radiation dose received and the fraction of cells that survive that dose. Since the term "survival" can be interpreted in many different ways, it is necessary to clarify how it will be defined in this study. Cell survival for certain differentiated cells, such as nerve, muscle, or secretory cells, can be described as loss of a specific function [1]. Survival for proliferating cells can be described as a loss of the ability to sustain successful mitotic activity. This loss of reproductive integrity is known as *reproductive death*. This ability is measured by whether or not a single cell (plated *in vitro*) can develop into a large clone, or colony. (Since radiation-damaged cells may struggle through a few mitoses, it is necessary to define a colony as a certain expected number of cells, given a length of time.) This is of particular interest when dealing with tumor cells, since if the cells are rendered incapable of reproduction, growth of the tumor will cease. Therefore this study will use reproductive integrity, (or the loss thereof), as a measure of cell survival.

Cell survival curves are generally limited to proliferative cells, for it is the dividing cells of an organism that comprise the stem-cell compartment, and in whole-body radiation exposure whether or not the stem cells survive determines the outcome of the individual [2]. Proliferative cells have a mean lethal dose of ~2 Gy (200 rads), while a dose of 100 Gy (10,000 rads) is usually necessary to destroy the function of differentiated cells [1].

In order to develop a reasonable understanding of cell survival curves, it is useful to note the steps necessary to generate these curves in an experimental situation. Established cell lines are almost always used in cell survival experiments, since many of the *normal* characteristics of the cells are well documented.

Cells from an actively growing stock culture are generally removed from their growing surface, or "farmed," by use of the chemical agent trypsin. Trypsinization removes the cells by dissolving and loosening the cell membrane. It is possible to over-trypsinize cells (noted by cell lysing), so the amount of time the cells are exposed to the trypsin is vital. The single cells are then suspended in an isotonic solution and counted using either a hemacytometer or an electronic counter. It is then possible to irradiate and subsequently seed plates with a known number of cells. The plates are then incubated for one to two weeks. Generally, surviving cells will divide and form large colonies, while radiation damaged cells will not. The colonies are then counted, and the number of colonies is compared to the number of cells plated.

However, since some surviving cells (even those not exposed to radiation) do not divide and form colonies, it is necessary to calculate what is known as a *plating efficiency* (PE). This is done by plating a known number of cells onto a plate that is not exposed to radiation, incubating the plate under the same conditions as for the irradiated cells, and counting the surviving colonies. These plates are generally used as the experimental controls. The plating efficiency (in percent) is therefore given by

$$PE = \frac{Colonies\ Counted}{Cells\ Seeded} \times 100$$

For example, if 200 cells were seeded (plated) and 140 survived to form colonies, the PE would be 70%. The plating efficiency then must be applied to each plate that has been irradiated in order to assess whether or not cell death is due to radiation damage or other factors. Other factors may include anything from poor growth medium, counting errors, or cell trauma through handling. The *surviving fraction* (S) of cells from each of the irradiated plates is then given by

$$S = \frac{Colonies\ Counted}{Cells\ Seeded\ x\ (PE/100)}$$

Therefore, if 1000 cells were seeded and 100 colonies counted (with a 70% PE), the surviving fraction would be 0.14, or 14%. Ideally, to make colony counting less of a chore, experimenters generally try to grow no more than 200 colonies per plate. In order to achieve this, it is necessary to seed many more cells at higher radiation doses as compared to lower doses. For example, say the PE is known to be 70% for a given cell line under certain experimental conditions. In order to achieve 200 colonies (on an unirradiated plate) it would be necessary to seed the plate with 285 cells. When plates are seeded prior to irradiation, a specific number of cells (depending on the amount and type of radiation administered) must be derived for each dose. The surviving fraction of cells for higher doses of radiation is often very low, and hundreds of thousands of cells are sometimes seeded to achieve 200 colonies.

These surviving fractions are then plotted on a log scale against radiation dose, and generally appear as illustrated in Figure 2-1.

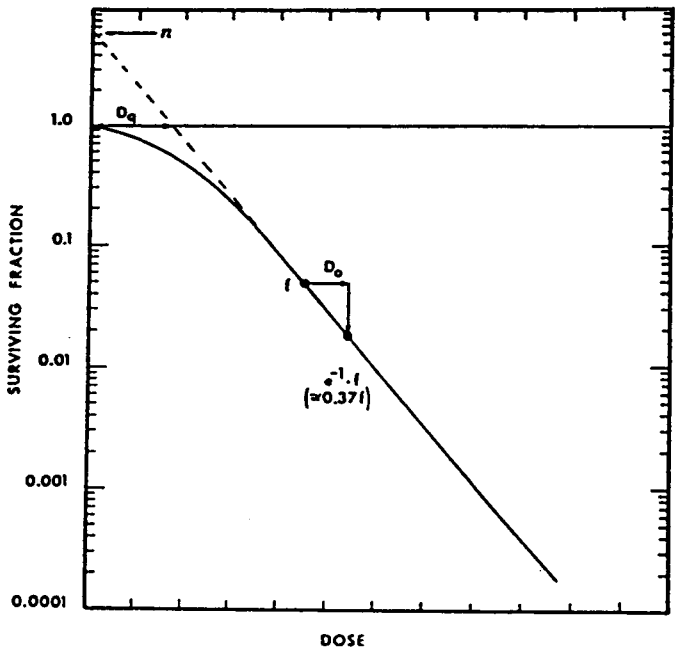

Figure 2-1 Dose-Survival Curve for Mammalian Cells
A typical low LET radiation survival curve illustrating the extrapolation number, n, the quasi-threshold dose, D_q, and the D_0, (also known as D_{37}). [3]

From the shape of a survival curve it is possible to note several things pertaining to the radiosensitivity of the cells involved, for the shape of the curve varies depending on the type of radiation to which the cells are exposed. For sparsely ionizing radiation (x-rays or gamma rays), the curve starts out at lower doses as a straight line with a slope of nearly zero (see Figure 2-2). As theories that will be discussed shortly will attain, this is due to the ability of cells to withstand higher doses of low LET radiation, (as compared to high LET radiation). As dose increases, the curve bends, extending over a few Gy (a few hundred rads). At high doses the curve straightens out and the surviving fraction can be measured as an exponential function of dose. For more densely ionizing radiation (high LET particles such as α-particles or low energy neutrons), a survival curve is

effectively a straight line from the origin. Survival in this case can therefore be approximated as an exponential function of dose for the entire curve [1].

While qualitatively assessing survival curves is relatively simplistic, describing the shape of survival curves based on the effects of radiobiological events is another matter.

2.2 Methods of Interpretation

Cell survival curves display the underlying relationship between radiation dose and biological effect. In order to interpret the results of these curves, both mathematical formulae and theoretical mechanics of action have been derived. Cell inactivation theories developed as a result of the known stochastic nature of energy absorption in biological material [3]. The most well-known of these theories is the Target Theory, which can be applied to both exponential and shouldered survival curves. Other theories include the Theory of Dual Radiation Action, the "Molecular Theory" of Cell Inactivation, and repair models (Q-Repair). Since it is not actually known which of these theories, if any, is correct, each of them will be discussed briefly. First, however, an overview of what information can be gained from survival curves is necessary.

The abbreviations D_0, D_q, and n (see Figure 2-1) are often used as a means of quantifying cell radiosensitivity. The term D_0 (often known as D_{37}) is the dose required, within the exponential region, to reduce the fraction of cells surviving from some value f to $e^{-1}f$ (~0.37f, hence the name); D_q (known as the *quasi-threshold* dose) refers to the width of the shoulder and corresponds to the value of the intercept of the extrapolated straight portion of the curve at the surviving fraction of 1.0; n is the extrapolation value of the intercept from the straight portion of the curve on the survival axis at zero dose.

The shapes of survival curves and the changes exhibited due to differing types of radiation have been a basis for constructing various mathematical models and theories concerning the biophysical mechanisms involved in cell killing, or inactivation processes.

2.2.1. Target Theory

The conceptual basis of target theory rests on the assumption that the observed biological effects are due to a single energy absorption event in the discrete target volume within a cell [3]. The target may be a whole cell, part of a cell, or a critical organ [4]. The assumption of a discrete sensitive volume, or target that must be inactivated to create the desired effect (whether or not it is valid), has been a dominant theme in radiobiology from the 1920s up to the present [3]. Since mammalian cell survival curves are of two shapes (exponential or sigmoid), there are two slightly different derivations.

Exponential Curves

The dose delivered is defined in terms of the number of inactivating hits per unit volume of irradiated material. In the sensitive volume, if the average hits per target (distributed randomly) is A, then the fraction of targets receiving exactly n hits can be represented by the Poisson formula

$$\frac{e^{-A} A^{n}}{n!}$$

If it is assumed that cell inactivation occurs following a single hit to the target, a biological statement of the survival fraction can be represented as

$$S = e^{-A}$$

If D_0 is the dose required to reduce cell survival from 1 to 1/e, and which gives, on average, one lethal event per target, then

$$S = ne^{-D/D_0}$$

Target theory in this regard seems fairly abstract, and mathematical. Biologically, however, it is an extremely complex process, and many factors, such as the differing levels of complexity of each of the cell structures, must be considered. If each of these targets is considered individually, a new formula can be derived, but still without information with regard to target size.

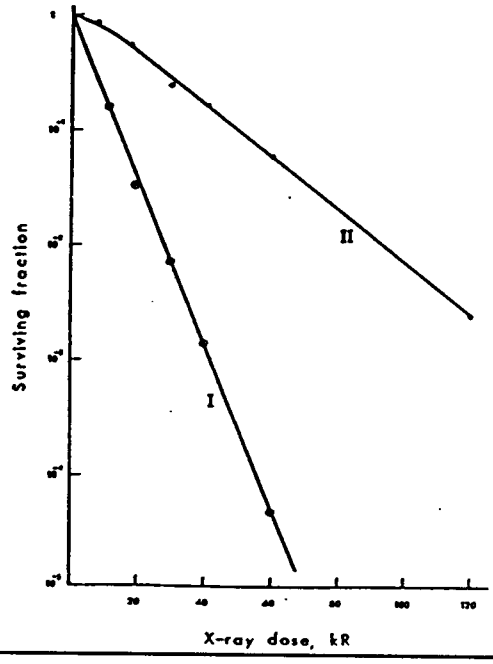

Figure 2-2 High LET vs Low LET Survival Curves for Mammalian Cells
Curve II illustrates a typical low LET radiation (X-rays in this case) shouldered survival curve. Curve I is exponential form the origin, typical of high LET radiation such as neutrons.

Shouldered Survival Curves

For a single-hit, multitarget model, the general formula for a cell survival curve with an initial slope of zero, a shoulder, and an exponential region is

$$S = 1-(1-e^{-D/D_0})^m$$

where m = the number of independent targets per cell requiring a hit for the cell to be inactivated, and assuming each of the m targets must be hit once for cell inactivation to occur. Mathematically, this formula works very well; however, physiologically m seems to depend heavily on the state of the cell, its stage in the cell cycle, and the conditions of irradiation [3].

In general, target theory has created a framework from which attempts are made to interpret the shapes of survival curves in biophysical terms. However, since the cell's metabolic state and repair processes are not taken into consideration, it seems nearly impossible to make a biological translation of which mechanisms are responsible for cell inactivation versus cell survival.

2.2.2. The Theory of Dual Radiation Action

This model is based on the concept that it takes more than one hit per target to induce inactivation. This theory was developed by Kellerer and Rossi [5] to explain the relationship between RBE (Relative Biological Effectiveness) and radiation dose for high LET radiation. They arrived at the equation of the form

$$S = e^{-\alpha D - \beta D^2}$$

where α refers to the probability of an effect being caused by a single track, (hit), while β refers to the probability that an effect was caused by two tracks. This gives a survival curve which has a shoulder but which is continuously bending. Although this method of interpretation has been shown to work well in certain circumstances, the general validity of this theory has been questioned. However, recent studies involving irradiation with deuteron pairs versus single deuterium ion beams have shown that in fact greater cell killing does occur when irradiating with ion pairs [3].

2.2.3. The "Molecular Theory" of Cell Inactivation

The concept of this theory, developed by Chadwick and Leenhouts [6], is also based on the idea that more than one hit per target is necessary for cell inactivation. However, the "Molecular Theory" assumes that all cell inactivation is caused by the induction of unrepaired double-strand breaks in DNA [3]. With low LET radiation, it is thought that the breaks can result from either one hit or two separate hits near one another on the complementary strands of DNA. From these assumptions a relationship identical to that of dual radiation action gives

$$S = e^{-\alpha D - \beta D^2}$$

where here α refers to a single-strand break inactivation and β to a double-strand break inactivation. It is thought that for low LET radiations and doses greater than a few Gy, cell inactivation will occur predominately by single-strand breaks that, if repaired improperly, will become double-strand breaks. (Generally, it is thought that induction of

double-strand breaks from a single event is cause for cell inactivation.) Although the equation derived in this theory (and dual radiation) allows for a better fit to cell survival data, the basic assumptions to the "Molecular Theory" have also recently been open to doubt.

2.2.4. Repair Models

The repair theory for shouldered curves was first introduced by Powers [7]. It also involves the concept that cell killing is due to a multiplicity of ionizing events, only viewed in a slightly different way. According to this theory one damaging event can kill the cell if it is not repaired, or somehow rendered incapable of repair over a certain length of time [3]. From studies with ultrasoft X-rays, Goodhead et al. [8] proposed that for low LET radiation, lethal lesions are the result of small amounts of energy (up to 300 eV) in a few nm as a result of a one-hit action. The number of lesions produced is proportional to dose and the efficiency of production is proportional to LET [3]. The shoulder of the survival curve is the result of some of the lesions being repaired. This repair process is dose-dependent and is saturated at higher doses. This explanation of the shoulder of survival curves is also known as *Q-repair*. From repair models of this type, it is possible to postulate why both exponential and shouldered curves exist. With low LET radiation (shouldered curves) more repairs are possible at the lower doses, while high LET radiation (exponential curves) even at low doses allows little, if any, repair.

With these and other theories it is possible to fit survival curve data with a number of mathematical formulae. However, with the numerous subtleties in the biological function of cells, it is impossible to predict the mechanisms of action which cause cell

inactivation strictly in this manner. With the discovery of repair processes, such as the Q-factor, there is hope for improved, more biophysically oriented models.

2.3 References

1. Hall, E.J., Radiobiology for the Radiobiologist, Fourth Edition, J.B. Lippincott Company, Philadelphia, 1994, pp. 29-43.

2. Grosch, D.S., Biological Effects of Radiations, Academic Press, Inc., New York, NY, 1979, pp. 93-109.

3. Pizzarello, D.J., Ph.D., Radiation Biology, CRC Press, Boca Raton, FL, 1982, pp. 28-38, 72-78.

4. Casarett, A.P., Radiation Biology, Prentice-Hall, Inc., Englewood Cliffs, NJ, 1968, pp. 136-147.

5. Commitee for Radiation Oncology Studies (CROS), and its particle Subcommitee, "Proposal for a program in particle-beam radiation therapy in the U.S.," *Cancer Clinical Trials*, 1(3), 173, Fall 1978.

6. Chad, K.H., Leen, H.P., A molecular theory of cell survival, *Phys. Med. Biology*, 18, 78, 1973.

7. Powers, E.L., "Considerations of Survival Curves and Target Theory", *Phys. Med. Biology*, 7, 3, 1962.

8. Goodhead, D.T., Thacker, J., Cox, R., "Effectiveness of 0.3 keV carbon ultrasoft X-rays for the inactivation and mutation of cultured mammalian cells, *International Journal of Radiation Biology*, 36, 101, 1979.

CHAPTER 3. CELL SURVIVAL CURVE EXPERIMENTS

3.1 Materials and Methods

It should be noted that this survival curve experiment was done using *only* ^{60}Co gamma radiation, not neutrons. Therefore the cells were not incubated in a boron solution, since gamma rays would have the same effect on the cells whether or not boron was present. The purpose of a ^{60}Co survival curve is to provide a comparative curve against which to compare any other survival curves (of the same cell line) performed under different conditions or with other types of radiation. The results that follow will not be showing the BNCT effect, but rather the effect of ^{60}Co gamma rays on AtT-20 cells.

Glioma Cell Line

The Clone AtT-20, an ACTH secreting cell line, was cloned in October, 1966 by G. Sato and associates. The cells are derived from a mouse pituitary tumor originally established in LAFI mice by J. Furth, et al.[1]. The cells were cultured in Ham's F10 medium, 82.5%; horse serum, 15%; fetal bovine serum, 2.5%. This clone has been carried in culture without alternative animal passage and produces ACTH at a rate of ~1000 mU/mg of cell protein per week. An inoculum of 10^5 viable cells/ml will multiply four-fold in 10 days. These cells do not form monolayers, but instead tend to grow as small floating clusters. Cells appear small and rounded in solution, and slightly elongated when attached to a growing surface. ACTH production continues for at least 20 passages after recovery from the frozen state [2].

Experimental Design and Sample Preparation

AtT-20 cells were supplied to OSU through the Vollum Institute, Portland, OR. The cells were grown to near confluency in either T-75 or T-150 flasks. The cells were prepared into a single-cell suspension using 1 to 2 ml of trypsin and a 5 minute incubation at 37 °C. The cells were then centrifuged for 5 minutes to remove the residual trypsin. A dilution was then performed using Dulbecco's Modified Eagle Medium (D-MEM) to 20 ml. 100 µl was taken of the 20 ml solution and placed into 9.9 ml of isotonic solution. The cell mixture was then counted on a Coulter Counter. After determining cell density per ml, 2-3 ml of the diluted 20 ml cell solution was placed into a series of vials for irradiation by ^{60}Co gamma rays.

Irradiation Conditions

The irradiator used in the experiment was a 53 Curie source ^{60}Co Nuclear Systems/Budd (model R60124). When the sources are raised, the irradiator has both a low flux region, where the dose ranges from 19-65 cGy/min, and a high flux region with a dose range of 85-181 cGy/min. Due to the structure of the irradiator, the dose rate depends on the position of the sample, while the total dose depends on the length of time each sample is exposed to the source. The calibration for the irradiator is kept current through a computer program which automatically accounts for the decay of the source over time, and continually adjusts the exposure times necessary to achieve a desired dose.

The sample vials containing the AtT-20 cell solution were each placed separately into the bottom of the low flux region where they received approximately 60 cGy/min.

Individual total doses received for the 7 vials were 0 (control), 100, 200, 300, 400, 500, 600, and 800 cGy.

Table 3-1 shows relative exposure times necessary to achieve each dose. These times account for the "up" and "down" transit times for the source.

Table 3-1 ^{60}Co γ-ray Exposure Times

EXPOSURE (cGy) (bottom of the low flux chamber)	ELAPSED TIME (minutes)	(seconds)
100	1	28
200	3	15
300	5	02
400	6	49
500	8	36
600	10	23
800	13	56

Cell Plating

Immediately following irradiation, several dilutions were made (using DMEM) of each sample vial prior to cell plating. The goal of these dilutions was to arrive at a number of cells so that, when plated, 14 days later approximately 200 colonies would remain for each dose point, (assuming 70% plating efficiency). Following each final dilution, a count was made using the Coulter Counter to check plating accuracy, (except for experiment #1 at 600 and 800 cGy). For each of the three experiments the dilutions and cell plating were as follows:

Table 3-2 Experiment #1 Cell Plating

Stock Solution	Dose (cGy)	Goal # of cells to plate	Actual # of cells plated
320,000 cells/ml	0	300	375
"	100	300	320
"	200	300	320
"	400	600	750
"	600	4000	*
"	800	40,000	*
"	800	80,000	*

* Information not available

Table 3-3 Experiment #2 Cell Plating

Stock Solution	Dose (cGy)	Goal # of cells to plate	Actual# of cells plated
757,000 cells/ml	0	300	420
"	100	300	450
"	200	300	390
"	300	450	640
"	400	700	960
"	500	2300	3260
"	600	5000	6730
"	800	55,000	76,700

Table 3-4 Experiment #3 Cell Plating

Stock Solution	Dose (cGy)	Goal # of cells to plate	Actual # of cells plated
2,345,000 cells/ml	0	300	260
"	100	600	575
"	200	600	510
"	300	1200	910
"	400	3200	2460
"	500	15,000	9460
"	600	56,000	45,600
"	800	700,000	532,000

Following the final dilution, each of the samples was split into five separate 10 cm plating dishes, with the appropriate number of cells per dose point plated in each dish. The two main reasons for this step was 1) to test the accuracy of plating techniques, and 2) to ensure that no dose point would be eliminated should contamination occur. (Plates that became contaminated were eliminated from the experiment.) The Coulter Counter is accurate to a much higher degree than the pipettes used to draw the cells from the vials, so the *goal number* of cells to plate and the *actual number* of cells plated are different. The plates were then incubated at 37 °C for 14 days. The cell medium (D-MEM, 10% FCS + penn-strep) was changed every third day for the two week period.

Colony Counting

After 14 days, the remaining plates were removed from the incubator. The cells were drained of media and washed with phosphate buffered saline (PBS). A 10% formaldehyde solution was then placed into each plate for the purpose of "fixing" the cells to the plate. After rinsing with PBS a second time, a small amount of 5% Giemsa stain

was placed onto each plate, remaining in contact with the cells for approximately five minutes. The cells were then washed with doubly distilled water to remove the excess stain.

With the colonies now visible, representative plates for each dose point were examined under an Olympus (model CK 2) inverted microscope at high power to determine what a *viable* colony looks like to the naked eye. It was determined that a viable colony is generally a colony of 50 cells or more, a large percentage of which appear "normal".

The first set of plates (from experiment #1) was counted by stretching a piece of Parafilm over the underneath side of each plate, and with a permanent pen marking each colony as it was counted. This method seemed to work fine; however, the next two sets of plates (experiments #2 and #3) were counted using an automatic colony counter (BANTEX 900A). The counter set-up includes a 32 watt circular fluorescent light source, a 150 mm grid on which to set the plates, a 1.5X magnifier, and a porous tip electronic pen that not only marks each colony, but automatically registers a count, sounding a tone for each, when contact with the counting surface is made. This method was time-saving as well as being highly accurate and precise.

3.2 Results

Colony Growth and Development

A total of 40 plates were seeded with cells following irradiation (five per dose point) and incubated for 14 days. Each of the plates was examined daily to determine if any contamination were present. During the latter phases of growth, approximately 25%

of the plates showed some form of contamination. If the contamination was minimal, the plates could often be saved, but several plates were completely overgrown and had to be thrown out. Since contamination was kept under control to as great a degree as possible, each data point was accurately represented, with a few exceptions. The 14-day growth period seemed ideal, since within that time the colonies had grown large enough to be seen with the naked eye.

Colony Counting

Each of the five plates per dose point was counted and an average number of colonies per dose point calculated. The % survival (normalized to control) was calculated by dividing the % survival for each of the dose points by the % survival for the control, i.e., by the *plating efficiency*. The results for each of the experiments were as follows:

Table 3-5 Experiment #1 Results

Dose (cGy)	# of cells plated	Ave. # colonies	% survival	% survival normalized to control
0	365	220±09	60.3	1.00
100	320	194±10	60.6	1.00
200	320	183	57.2	0.95
400	750	167	22.2	0.37
600	4000	158±11	3.9	0.065
800	40,000	142±11	0.35	0.0058

Table 3-6 Experiment #2 Results

Dose (cGy)	# of cells plated	Ave. # colonies	% survival	% survival normalized to control
0	420	279±20	66.4	1.00
100	450	151±21	33.6	0.51
200	390	130±20	33.3	0.50
300	640	107±19	16.7	0.25
400	960	60±15	6.3	0.095
500	3260	43±11	1.3	0.020
600	6730	24±11	0.31	0.0047
800	76,700	11±07	0.014	0.00021

Table 3-7 Experiment #3 Results

Dose (cGy)	# of cells plated	Ave. # colonies	% survival	% survival normalized to control
0	260	212±17	82.2	1.00
100	575	417±24	72.5	0.88
200	510	275±24	54.1	0.66
300	910	122±20	13.4	0.16
400	2460	190±23	7.7	0.094
500	9460	264±22	2.8	0.034
600	45,600	238±26	0.5	0.006
800	532,000	219±25	0.04	0.0005

Survival Curves

The three survival curves generated from these colony counts are typical of low LET radiation (X-ray or gamma ray) exposure. There is a near zero slope region for low doses, a shoulder, and an exponential region for high doses (See Figures 3-1, 3-2 and 3-3).

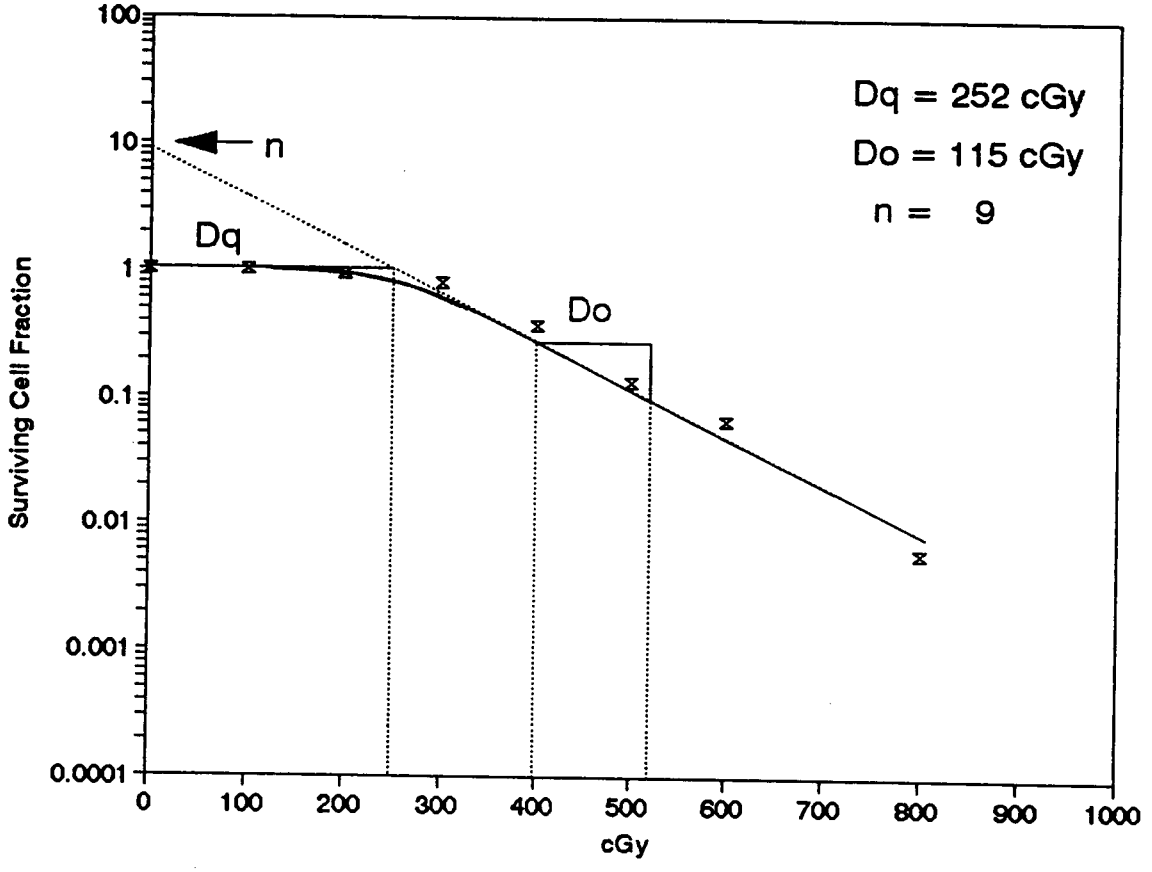

Figure 3-1 ^{60}Co Experiment 1 AtT-20 Cell Survival Curve

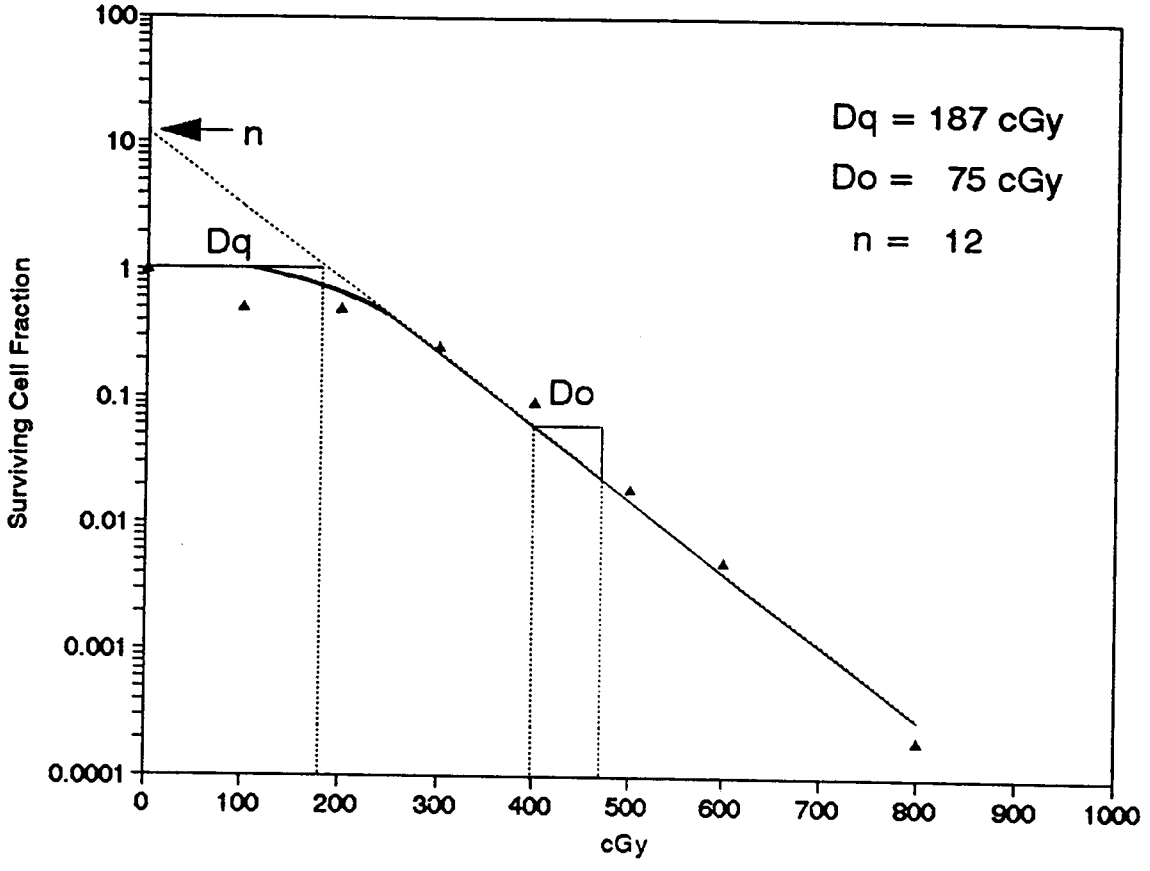

Figure 3-2 ^{60}Co Experiment 2 AtT-20 Cell Survival Curve

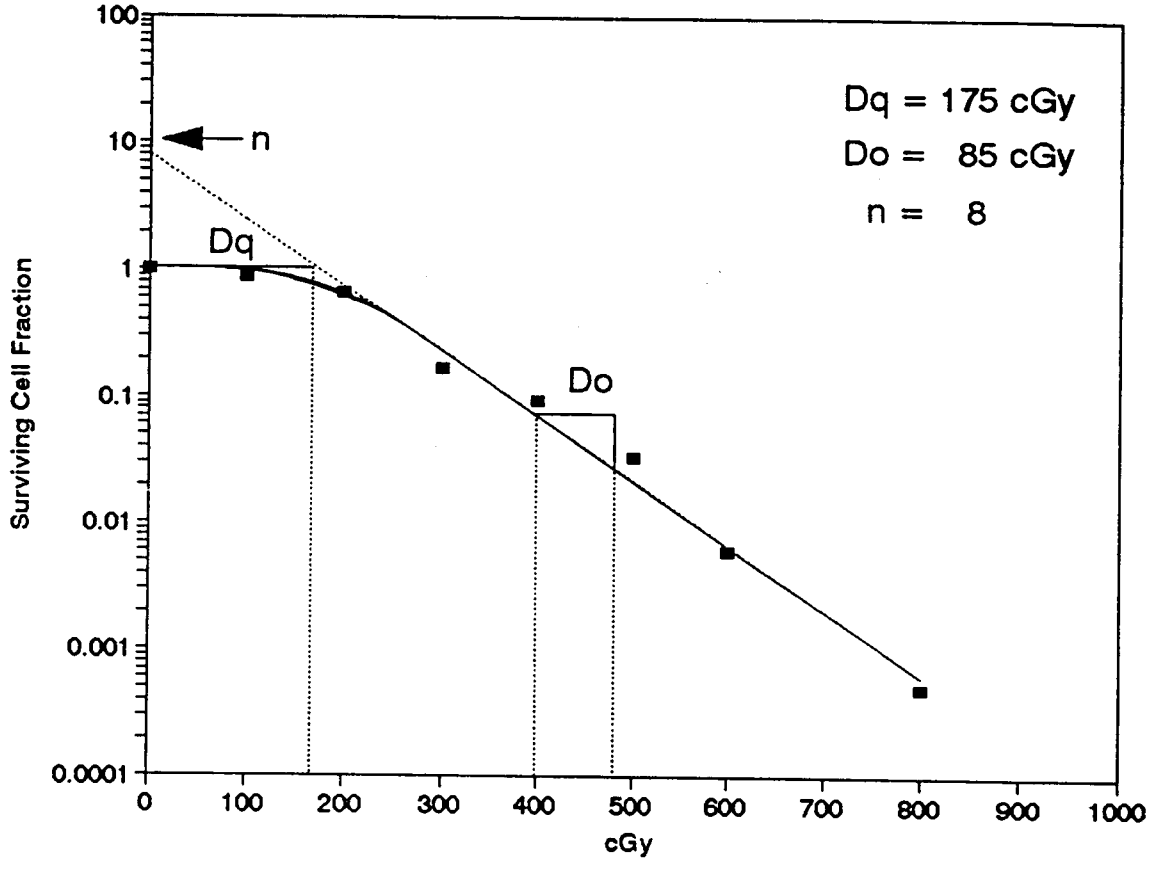

Figure 3-3 ^{60}Co Experiment 3 AtT-20 Cell Survival Curve

Table 3-8 shows the relationship between each of the three parameters (D_0, D_q, and n) for each of the three experiments.

Table 3-8 Comparative Cell Survival Curve Parameters for Experiments 1, 2, and 3

Experiment #	D_q (cGy)	D_o (cGy)	n
1	252	115	9
2	187	75	12
3	175	85	8

As can be noted from Figures 3-1, 3-2 and 3-3, (as well as from Table 3-8), the parameters of the three curves are relatively close in numerical value. Figure 3-4 shows the relationship between all three cell survival curves, and despite their differences, the slope of each is quite consistent with the others. However, since curves 2 and 3 show a higher degree of similarity to each other than to curve 1, Figure 3-5 is a combined exponential fit of curves 2 and 3. This final curve is therefore representative of a low LET radiation cell survival curve for the AtT-20 cell line.

Calculation of Statistical Errors

Calculation of the statistical errors for curves 2 and 3 was done through the use of a binomial distribution, where the statistical error per dose point is shown by

$$\frac{\sqrt{qpn}}{n}$$

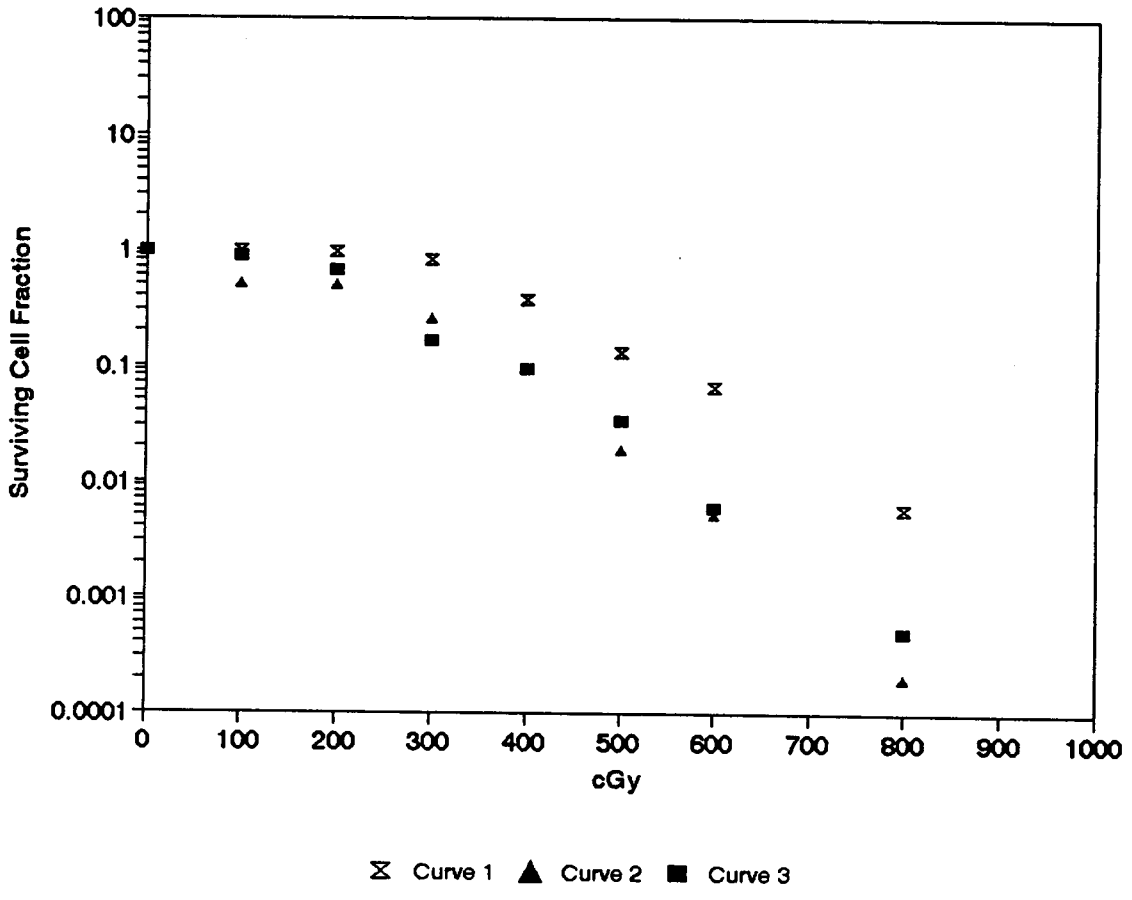

Figure 3-4 ^{60}Co AtT-20 Cell Survival Curves 1, 2 & 3

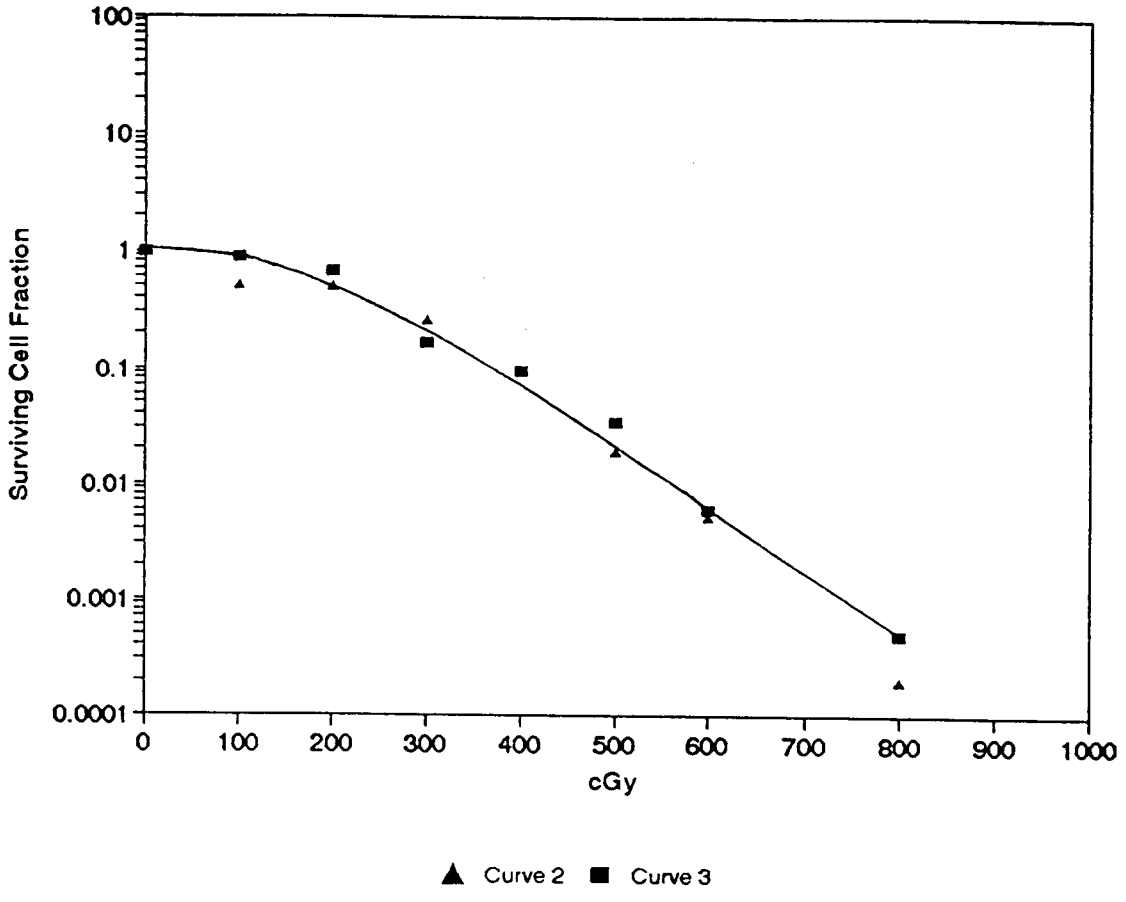

Figure 3-5 ^{60}Co AtT-20 Cell Survival Curve
(an exponential fit between curves 2 and 3)

where

$$p = \frac{\textit{the total number of colonies per dose point}}{n}$$

$$q = (1 - p)$$

$$n = \textit{the total number of cells plated per dose point}$$

If the formula is written as

$$p \pm \sqrt{(1-p)(\textit{number of colonies})}$$

it can be noted that as p gets very small, the error approaches

$$\sqrt{\textit{number of colonies}}$$

The determination that a binomial distribution was appropriate was made upon evaluation of the experiment:

1. The experiment consists of *n* identical trials.
2. Each trial results in one of two possible outcomes (success or failure).
3. The probability of success on a single trial is equal to p and remains the same from trial to trial. The probability of a failure is equal to (1-p) = q.
4. The trials are independent.
5. The random variable of interest is the number of successes observed during the n trials.

Table 3-9 contains the combined statistical errors for each dose point of experiments 2 and 3.

Table 3-9 The Combined Statistical Errors of Experiments 2 and 3

Dose (cGy)	Error (1σ)
0	4.55×10^{-3}
100	3.87×10^{-3}
200	3.70×10^{-3}
300	1.95×10^{-3}
400	9.59×10^{-4}
500	2.83×10^{-4}
600	5.08×10^{-5}
800	4.93×10^{-6}

3.3 Discussion

The OSU BNCT ^{60}Co survival curve experiments were carried out to demonstrate the effects of various doses of low LET radiation (X-rays or gamma rays) on a particular mammalian cell line. According to theories mentioned previously, survival curves of this nature should be of the sigmoid shape, with a zero-slope region, a shoulder and an exponential region. What was seen in the experiments was in fact a very reasonable representation of a low LET radiation survival curve. The results were quite repeatable, with slight exception to curve #1.

In the first experiment six dose points were measured, which left a few areas of the curve slightly open to suggestion. While the curve definitely tends to follow the shape of a low LET survival curve, viable plates for two of the dose points (200 and 400 cGy) were reduced to one plate due to contamination. Statistically, these points are not

extremely meaningful. However since both points fall within the general shape of the curve, they are assumed to be close to what an average of the dose point might have been. In experiment 2, two additional dose points (300 and 500 cGy) were included to smooth out the curve. These dose points proved to be quite informative and were also included in experiment 3.

The cell handling techniques also improved somewhat in the later experiments. For example, trypsinization in the first experiment did not seem complete, and the cells remained in clusters after being removed from the flasks. This could explain the difference in the order of magnitude of cell killing observed between the first experiment and the second two. Since the cells remained in clusters throughout the experiment, they were therefore irradiated as clusters. When irradiated, a cluster of cells would not react the same as a single cell. It would in fact act as a very resistant cell, since it would undoubtedly take many more hits to inactivate an entire cluster than it would to kill a single cell. These clusters, when plated, would therefore have a much greater chance of survival than a single cell, since any one surviving cell could form a colony. It is believed to be mainly for this reason that the first curve shows differing results from the second and third curves.

In addition, some of the equipment used in the first experiment was not as technologically advanced as in the later experiments. For example, the laminar flow hood under which the cells were handled did not have an ultraviolet lamp installed during the first experiment. (UV-C emitting lamps serve as an extra precaution against any spores or other contaminants that may enter the hood when its filter system is not in use.) It is

possible that the decreased amount of contamination seen in experiments 2 and 3 was due to the addition of this lamp. A propane gas flame was also installed prior to the second and third experiments. The tops of all bottles, flasks and the tips of pipettes were flamed before coming in contact with the cells. A vacuum system was also created and used for the purpose of quickly, safely and completely removing liquids from the cells, (e.g., cell media changes, cell staining, etc.). Liquid removal in the first experiment consisted of hand pipetting into a waste receptacle.

Colony counting changed drastically between the first and second two experiments. As mentioned before, the original method used consisted of a piece of parafilm stretched across the underside of the plates, and marking off colonies one at a time with a permanent marker. Although this method did seem to be fairly accurate, it would have been more so had a light source (other than room light) been availalble. The colony counter used in the second and third experiments included a bright light source, a counting grid, a magnifier, and an electronic pen which marked and counted simultaneously. It is not difficult to believe that this method was more accurate.

Although the second and third curves look to be nearly identical on paper, there were some differences in cell plating techniques between the two. In the second experiment, a slightly lower number of cells was plated per dose point than would have been ideal. Since the cells irradiated in the second experiment were completely trypsinized into a single-cell solution, the the kill ratio between cells plated and cells surviving increased more than anticipated. Therefore, the number of colonies per plate was slightly lower than expected. However, for the final experiment a much greater

number of cells was seeded per plate in order to arrive at approximately a 200 colony per plate number.

3.4 References

1. Proc. Soc. Exp. Biol. Med. 84: 253-254, 1953.

2. American *Type Culture* Collection, *Catalog of Cell Lines and Hybridomas*, 7th ed., 1992, ATCC CCL89, p. 54.

CHAPTER 4. CONCLUSIONS AND RECOMMENDATIONS

This chapter consists of a brief explanation of future plans for cell survival curves involving demonstration of a BNCT effect, as well as a general summary of the ^{60}Co cell survival curve experiments.

4.1 Future Survival Curve Experiments

Since the completion of AtT-20 ^{60}Co survival curves, procedures have begun for determining cell survival curves in the Oregon State TRIGA Reactor (OSTR). (The OSTR is a 1.1 MW Mark II research reactor.) The basic cell procedures will involve a short incubation in a solution containing a ^{10}B cage and hormone conjugate (as described previously). To determine a BNCT effect, the cells incubated in the ^{10}B solution will be compared to a control group incubated in a non-conjugated solution, but exposed to the identical neutron field, as well as a control group not incubated nor exposed to neutrons. The exposures will consist of 1, 2, 3, 4 and 5.5 MW-minutes in the thermal column of the reactor. The thermal column is an area of the reactor where the potential exists for maximal thermal neutron flux with a minimal epithermal and fast neutron component, as well as a relatively low gamma ray flux.

There have been many experiments in the OSTR involving boronylated AtT-20 cells, and a BNCT effect has been observed [1]. However, the task at hand is to generate cell survival curves demonstrating the BNCT effect.

4.2 Summary

With successful human clinical trials in Japan, hope has been renewed in BNCT as an alternative treatment for cancer. Originally thought to be useful in treating deep-seated gliomas and malignant melanomas, continuing research has provided some initial evidence favoring the use of BNCT in many other types of neoplasms, specifically breast, prostate, and endocrine cancers. OSU researchers, in collaboration with OHSU, are currently determining the efficacy of BNCT as a treatment for pituitary tumors, an endocrine cancer.

In order to clearly demonstrate a BNCT effect, it is necessary to generate cell survival curves through *in vitro* cell irradiations with neutrons. It is also necessary to show a comparitive curve generated through *in vitro* cell irradiations with ^{60}Co gamma rays, a low LET radiation.

A cell survival curve is a method of demonstrating the biological effects of radiation through *in vitro* irradiation of cells. Generally a number of dose points are covered (including 0), and as dose increases, cell survival decreases. The shape of these curves is of two basic forms: *exponential*, seen as a result of high LET radiation such as neutrons, and *shouldered*, typical of low LET radiation such as ^{60}Co gamma-rays. Several theories exist which attempt to explain the radiobiological phenomena involved in cell survival curve interpretation. The internal mechanisms responsible for whether or not cells survive irradiation are complex, and whether any of the theories is correct is not known. However, predictability in cell lines in response to specific radiations can be shown through the cell survival curve.

With the completion of the ^{60}Co cell survival curves, and the results thereof, the OSU/OHSU BNCT project will next focus on generating cell survival curves demonstrating a BNCT effect.

4.3 References

1. Albertson, B. D., Millan M. A., Binney, S. E., Willeke, G. B., Martsolf, S. W., Johnson, J. E., Loriaux, D. L., "The Use of Boron Neutron Capture Therapy for the Treatment of Pituitary Tumors," *Advances in Neutron Capture Therapy*, edited by A. H. Soloway *et al.*, 1993, pp. 623-628.

BIBLIOGRAPHY

Albertson, B. D., Millan, M. A., Binney, S. E., Willeke, G. B., Martsolf S. W., Johnson, J. E., Loriaux, D. L., " The Use of Boron Neutron Capture Therapy for the Treatment of Pituitary Tumors," *Advances in Neutron Capture Therapy*," edited by A. H. Soloway *et al.*, 1993, pp. 623-628.

Amaldi, E., D'Agostino, O., Fermi, E., Pontecorvo, B., Rasetti, F., Segre, E., (1935), "Artificial radioactivity produced by neutron bombardment" - II. *Proceedings of the Royal Society of London*, A., **149**, 522-558.

American *Type Culture* Collection, *Catalog of Cell Lines and Hybridomas*, 7th ed., 1992, ATCC CCL89, p. 54.

Barth, R.F., Soloway, A.H., Fairchild, R.G., "Boron Neutron Capture Therapy for Cancer," *Cancer Research*, 50, 1990, pp. 1061-1070.

Barth, R.F., Soloway, A.H., Fairchild, R.G., "Boron Neutron Capture Therapy for Cancer," *Scientific American*, Oct. 1990, pp. 100-106.

Campbell, M.J., Vermeir, G., Dams, R., "Influence of Chemical Species on the Determination of Mercury in a Biological Matrix (Cod Muscle) Using Inductively Coupled Plasma Mass Spectrometry," Journal of Analytical Atomic Spectrometry, vol.7, June, 1992, pp. 617-621.

Casarett, A.P., Radiation Biology, Prentice-Hall, Inc., Englewood Cliffs, NJ, 1968.

Chad, K.H., Leen, H.P., A molecular theory of cell survival, *Phys. Med. Biology*, 18, 78, 1973.

Commitee for Radiation Oncology Studies (CROS), and its particle Subcommittee, "Proposal for a program in particle-beam radiation therapy in the U.S.," *Cancer Clinical Trials*, 1(3),173, Fall 1978.

Durrant, S.F., "Inductively Coupled Plasma-Mass Spectrometry for Biological Analysis," *Trends in Analytical Chemistry*, II, 1992, pp. 68-73.

Farr, L.E., Robertson, J.S., "Neutron capture therapy," In: *Handbuch der Medizinische Radiologie*, Heidelberg: Springer, 1970, pp. 68-92.

Fermi, E., (1939), "Artificial radioactivity produced by neutron bombardment," In: *Les Prix Nobel en 1939*. Edited by M.A. Holmberg, Stockholm: Norstedt and Soner.

Fermi, E., Amaldi E., D'Agostino O., Rasetti F., Segre, E., (1934), "Artificial radioactivity produced by neutron bombardmant," *Proceedings of the Royal Society of London*, A, **146**, 483-500.

Goldhaber, M., (1986), Introductory remarks, In: Proceedings of a Workshop on Neutron Capture Therapy, Reports BNL-51994, Edited by R.G. Fairchild and V.P. Bond, Upton, NY: Brookhaven National Laboratory, pp. 1-2.

Goodhead, D.T., Thacker, J., Cox, R., "Effectiveness of 0.3 keV carbon ultrasoft X-rays for the inactivation and mutation of cultured mammalian cells, *International Journal of Radiation Biology*, 36, 101, 1979.

Gregorie, D.C., "Determination of Borons in Fresh and Saline Waters by Inductively Coupled Mass Spectrometry," *Journal of Analytical Atomic Spectrometry*, (vol.5) Oct. 1990, pp. 623-626.

Grosch, D.S., Biological Effects of Radiations, Academic Press, Inc., New York, NY, 1979, pp. 93-109.

Hall, E.J., Radiobiology for the Radiobiologist, Fourth Edition, J.B. Lippincott Company, Philadelphia, 1994, pp. 29-43.

Hatanaka, H., Introduction, In: *Boron-Neutron Capture Therapy for Tumors*, Edited by H. Hatanaka, Niigata, Japan: Nishimura, 1986, pp. 1-28.

Hatanaka, H., Urano, Y., Eighteen autopsy cases of malignant brain tumors treated by boron neutron capture therapy between 1968 and 1985. In: Boron Neutron Capture Therapy for Tumors, Edited by H. Hatanaka, Niigata, Japan: Nishimura, 1986, pp. 381-416.

Knoth, W.H., Sauer, J.C., Eng land D.C., Hertler, W.R., Muetterlies, E.L., (1964), Chemistry of borons, XIX. Derivative chemistry of $B_{10}H_{10}^{-2}$ and $B_{12}H_{12}^{-2}$, *Journal of the American Chemical Society*, **86**, 3973-3983.

Kruger, P .G., (1940), "Some biological effects of nuclear disintegration products on neoplastic tissue," *Proceedings of the National Acadamy of Sciences of the USA*, **26**, 181-192.

Locher, G. L., (1936), "Biological effects and therapeutic possibilities of neutrons," *American Journal of Roentgenology*, **36**, 1-13.

Matsumoto,T., "Transport Calculations of the Influence of Physical Factors on Depth-Dose Distributions in Boron Neutron Capture Therapy," *Physics, Medicine and Biology*, **35**, 1990, pp. 971-978.

Miller, H.C., Miller N.E., Muetterties, E.L., (1963), "Synthesis of polyhedral boranes," *Journal of the American Chemical Society*, **85**, 3885-3886.

Pizzarello, D.J., Ph.D., Radiation Biology, CRC Press, Boca Raton, FL, 1982, pp. 28-38, 72-78.

Powers, E.L., "Considerations of Survival Curves and Target Theory," *Phys. Med. Biology*, 7, 3, 1962.

Proc. Soc. Exp. Biol. Med. 84: 253-254, 1953.

Slatkin, D.N., "A History of Boron Neutron Capture Therapy Of Brain Tumors," *Brain*, **114**, 1991, pp. 1609-1629.

Stranathan, J.D., (1942), *The 'Particles' of Modern Physics*, New York: Blakiston, pp. 386-402.

Thapar, K., Kovacs, K., Laws, E.R., Muller, P.J., "Pituitary Adenomas: Current Concepts in Classification, Histopathology, and Molecular Biology," *The Endocrinologist* 3(1): 39-57, 1993.

Ungerer, A., A Description of ICP-MS, College of Oceanography and Atmospheric Sciences, Oregon State University, 1993.